

## Development of the charge exchange recombination spectroscopy and the beam emission spectroscopy on the EAST tokamaka)

Y. Y. Li, J. Fu, B. Lyu, X. W. Du, C. Y. Li, Y. Zhang, X. H. Yin, Y. Yu, Q. P. Wang, M. von Hellermann, Y. J. Shi, M. Y. Ye, and B. N. Wan

Citation: [Review of Scientific Instruments](#) **85**, 11E428 (2014); doi: 10.1063/1.4890408

View online: <http://dx.doi.org/10.1063/1.4890408>

View Table of Contents: <http://scitation.aip.org/content/aip/journal/rsi/85/11?ver=pdfcov>

Published by the [AIP Publishing](#)

---

### Articles you may be interested in

[Design of charge exchange recombination spectroscopy for the joint Texas experimental tokamaka\)](#)  
Rev. Sci. Instrum. **85**, 11E421 (2014); 10.1063/1.4891705

[High spatial and temporal resolution charge exchange recombination spectroscopy on the HL-2A tokamak](#)  
Rev. Sci. Instrum. **85**, 103503 (2014); 10.1063/1.4897186

[Charge exchange recombination spectroscopy on fusion devices](#)  
AIP Conf. Proc. **1438**, 189 (2012); 10.1063/1.4707876


[Enhanced core charge exchange recombination spectroscopy system on Joint European Torus](#)  
Rev. Sci. Instrum. **77**, 10F102 (2006); 10.1063/1.2222170

[Carbon ion plume emission produced by charge exchange with neutral beams on National Spherical Torus Experiment](#)  
Rev. Sci. Instrum. **77**, 10E902 (2006); 10.1063/1.2217012

---



**Does your research require low temperatures? Contact Janis today.  
Our engineers will assist you in choosing the best system for your application.**



- 10 mK to 800 K
- LHe/LN<sub>2</sub> Cryostats
- Cryocoolers
- Magnet Systems
- Dilution Refrigerator Systems
- Micro-manipulated Probe Stations

[sales@janis.com](mailto:sales@janis.com)   [www.janis.com](http://www.janis.com)  
**Click to view our product web page.**

# Development of the charge exchange recombination spectroscopy and the beam emission spectroscopy on the EAST tokamak<sup>a)</sup>

Y. Y. Li,<sup>1</sup> J. Fu,<sup>1</sup> B. Lyu,<sup>1,b)</sup> X. W. Du,<sup>2</sup> C. Y. Li,<sup>2</sup> Y. Zhang,<sup>1,2</sup> X. H. Yin,<sup>1,2</sup> Y. Yu,<sup>2</sup> Q. P. Wang,<sup>2</sup> M. von Hellermann,<sup>3</sup> Y. J. Shi,<sup>2,4</sup> M. Y. Ye,<sup>1,2</sup> and B. N. Wan<sup>1,2</sup>

<sup>1</sup>*Institute of Plasma Physics, Chinese Academy of Sciences, Hefei, Anhui 230031, China*

<sup>2</sup>*School of Nuclear Science and Technology, University of Science and Technology of China, Hefei, Anhui 230026, China*

<sup>3</sup>*FOM-Institute for Plasma Physics "Rijnhuizen," Association EURATOM, Trilateral Euregio Cluster, 3430BE Nieuwegein, The Netherlands*

<sup>4</sup>*WCI for Fusion Theory, National Fusion Research Institute, 52 Eoeun-Dong, Yusung-Gu, Daejeon 305-333, South Korea*

(Presented 4 June 2014; received 1 June 2014; accepted 5 July 2014; published online 20 August 2014)

Charge eXchange Recombination Spectroscopy (CXRS) and Beam Emission Spectroscopy (BES) diagnostics based on a heating neutral beam have recently been installed on EAST to provide local measurements of ion temperature, velocity, and density. The system design features common light collection optics for CXRS and BES, background channels for the toroidal views, multi-chord viewing sightlines, and high throughput lens-based spectrometers with good signal to noise ratio for high time resolution measurements. Additionally, two spectrometers each has a tunable grating to observe any wavelength of interest are used for the CXRS and one utilizes a fixed-wavelength grating to achieve higher diffraction efficiency for the BES system. A real-time wavelength correction is implemented to achieve a high-accuracy wavelength calibration. Alignment and calibration are performed. Initial performance test results are presented. © 2014 AIP Publishing LLC. [<http://dx.doi.org/10.1063/1.4890408>]

## I. INTRODUCTION

Charge eXchange Recombination Spectroscopy (CXRS) has been widely developed as a tool to measure localized ion temperature, plasma rotation, and the impurity densities in magnetically confined plasma devices.<sup>1,2</sup> Radial profiles of impurity densities can be obtained by combining CXRS and beam emission spectroscopy (BES) without requiring absolute intensity calibration and knowledge of neutral beam density.<sup>3-6</sup> BES can also provide information on the beam attenuation and beam component. The poloidal rotation can also be calculated from the poloidal asymmetries between the toroidal rotations on the high- and low-field sides of the plasma in addition to the direct measurement using the vertical CXRS views.<sup>7</sup> Recently, a neutral beam with positive ion sources has been installed on EAST.<sup>8</sup> The available power of neutral beam injection (NBI) is 2–4 MW, with injection energies of 50–80 keV for deuterium neutrals. This paper describes the details of the hardware, alignment and calibration associated with the viewing optics and the spectrometers for CXRS and BES on EAST.

## II. VIEWING GEOMETRY

The geometric arrangement of the heating neutral beams and the periscope lines of sight for the core and edge CXRS

views are shown in Fig. 1. NBI will be launched from A port for plasma heating, current drive, and diagnostic support. Each neutral beam has two sources, one pointing more tangentially to the toroidal direction than the other. The periscope lines of sight are situated at the position near the plasma midplane and aligned to the more tangential beam from D port.

Two independent and identical periscopes are used to view the core and edge of the EAST plasma using collection and fiber optics (see Fig. 1). The core CXRS covers a radial region from  $R = 1.55$  m (High magnetic side) to  $R = 2.33$  m (Separatrix) on the midplane ( $R$  is the coordinate along the major radius), and retains the ability to deduce the poloidal rotation from the toroidal rotation indirectly. The core CXRS has a radial resolution  $\Delta r = 0.5$ – $3$  cm (core to edge), which is unfavorable for the plasma of pedestal region. The radial resolution of edge CXRS is reduced down to  $0.7$  cm, complimenting the core CXRS. The BES shares the identical viewing optics with the core CXRS. Dedicated views are also arranged to measure the background emission. This viewing lens and the spectrometer are shared by the Edge Doppler Diagnostic,<sup>9</sup> which measures emission from LiI, LiII, HeII, CIII, and ArII and so on. EAST NBI can be modulated in its power, and the modulation frequency is up to 100 Hz, so it provides the ability to subtract the passive lines using the beam modulation. CXRS measurements on EAST are designed to make both on typical ion species, such as carbon, lithium (CVI: 529.1 nm;<sup>10,11</sup> LiIII: 449.9 nm,<sup>12</sup> 516.7 nm<sup>13</sup>), as well as on puffed impurity ion species, such as argon, neon, and helium (ArXVI: 436.5 nm; ArXVIII: 522.4 nm; NeX: 524.9 nm; HeII: 468.6 nm).<sup>11</sup>

<sup>a)</sup>Contributed paper, published as part of the Proceedings of the 20th Topical Conference on High-Temperature Plasma Diagnostics, Atlanta, Georgia, USA, June 2014.

<sup>b)</sup>Author to whom correspondence should be addressed. Electronic mail: blu@ipp.ac.cn

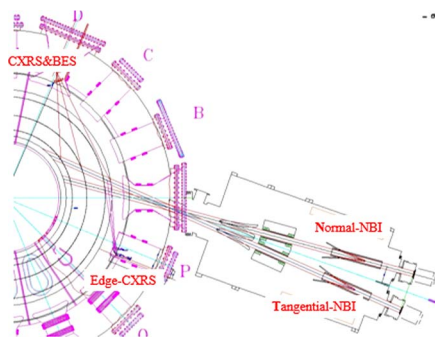


FIG. 1. Layout of the CXRS and BES on EAST.

## A. Collection optics and fibers

The collection optics consists of a quartz reflecting mirror, a telecentric imaging lens, and an array of quartz fibers. Each of these components is selected to provide good transmission and sensitivity as well as achromatic imaging in the wavelength range of 350–700 nm. Since the plasma sampling positions along the neutral axis are not perpendicular to the optical axis, the fiber holder located at the image plane is curved and tilted to match the image plane of the periscopes and to assure that the  $f$  number ( $f/2.27$ ) of each fiber is filled.

Figure 2 shows the images of the fiber optics (circles) along the neutral beam for core CXRS. An array of 70 horizontal channels and 4 vertical channels is used for the toroidal lines of sights. The vertical separation between the images of the fibers is only about 1.5 cm, which is considerably smaller than the height of the heating beam ( $\sim 48$  cm). The fibers in the same horizontal position can be binned together on the CCD detector to improve the signal-to-noise ratio as well as for the high temporal resolution. The 30 fibers shown by red circles are used for the core measurements. Ten channels, indicated by blue circles, are for BES system. There are also 32 pairs of chords that observe a region of  $\sim 18$  cm across the separatrix at the midplane.

Optical fibers with a 400  $\mu\text{m}$  core diameter are used for the core CXRS and BES. For the edge CXRS, 200  $\mu\text{m}$  diameter fibers are used. Pure quartz is adopted for the core and clad of the fibers in order to minimize radiation damage. The fiber bundles include three parts: (a) periscopes ( $\sim 5$  m);

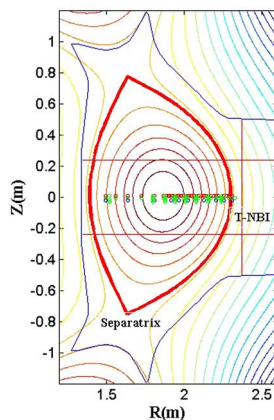


FIG. 2. Poloidal cross-section of toroidal views.

(b) periscopes to the diagnostic room ( $\sim 55$  m); and (c) spectrometers ( $\sim 2.4$  m). One end of the fibers of part (b) is connected to part (a) and the other end is connected to the fibers of part (c) which is aligned along the entrance slit of the spectrometers in the diagnostic room. The coating and jacket of part (b) and part (c) are made of nylon and polyurethane, respectively, to avoid snapped fibers as well as to prevent the electromagnetic interference. The fibers are connected to each other via Sub Multi Assembly (SMA) connectors mounted in a patch panel. The typical transmittance for a 55 m length of fiber at 532 nm is about 60%, measured at a numerical aperture of 0.22.

## B. Spectrometers and detectors

The collected light of core CXRS is transmitted to a high-throughput  $f/2$  lens-based spectrometer, which utilizes a fixed two-entrance-slits, two commercial lenses (Canon EF200mm  $f/2L$ ), and a movable grating with 2160 grooves/mm (see Fig. 3(a)). The entrance slit of the spectrometer is typically set to a width of 50  $\mu\text{m}$ . Using this slit and at the central wavelength of 529.05 nm, the instrument width of this system is between 0.059 and 0.061 nm depending on the spectrometer channel. The dispersion varies from 2.3 to 1.9 nm/mm at the spectral range 400–700 nm. The light from 30 fibers can be imaged simultaneously. A new frame-transfer back-illuminated CCD camera (Andor iXon Ultra 897) is coupled with the spectrometer. This detector has a popular back-illuminated  $512 \times 512$  array of  $16 \times 16$   $\mu\text{m}$  pixels and over-clocks readout to 17 MHz, resulting in an outstanding 56 fps (full frame). The vacuum quartz window is coated with dual anti-reflective coating for 400–900 nm and can achieve 99% transmission at 600 nm. With on chip binning of 15 regions of interest, the minimum integration time of this system will be 3 ms. The maximum shift due to the image curvature<sup>14</sup> can be up to 3 pixel at a wavelength of  $\lambda = 533$  nm (Ne lamp), corresponding to an apparent velocity of  $\sim 59$  km/s.

Three channels (two are on the ends and the third one is in the middle of the fiber array) will be always connected to a calibration lamp to perform a real-time wavelength calibration on a shot-by-shot basis. In this way, the shift of the rest wavelength arising from changes in the air pressure, temperature, as well as mechanical vibration can be excluded.<sup>15</sup>

Ten 400  $\mu\text{m}$  fiber optics, dedicated to the measurements of BES, are connected to a Hollowspec spectrometer (shown in Fig. 3(b)), which is equipped with a fixed Volume Phase Holographic grating (VPH). The observed spectral region is

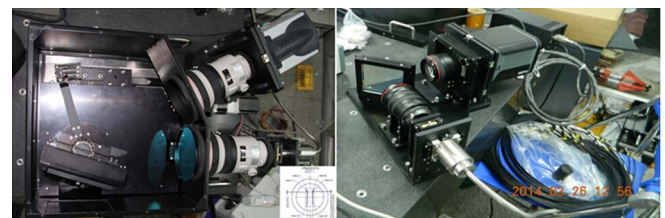


FIG. 3. Photograph of the spectrometers for the core CXRS (a) and for BES (b). Those are manufactured by University of Science and Technology of China (USTC).

647–659 nm, for which the grating efficiency is more than 70%. The spectrometer uses the standard lenses with a focal length of 135 mm at  $f/1.8$  and 85 mm focal length at  $f/1.2$  as the input lens and output lens, respectively. This arrangement demagnifies the image of the input fibers on the detector while preserving etendue and allows us to accept more fibers at the vertical entrance slit. Vertical binning of the fiber images due to a strong curvature of image plane will induce the loss of the spectral resolution ( $\sim 15\%$  for the outermost channel), so the image of the fibers will be calibrated before binning. The output of the spectrometer is imaged onto a CCD (Princeton Instruments ProEM) with a  $16 \times 16 \mu\text{m}$ ,  $512 \times 512$  pixels and a quantum efficiency of up to 90% at the wavelength of 656 nm. Exclusive eXcelon technology<sup>16</sup> can minimize the etaloning in the near-infrared (NIR) while keeping the high sensitivity. A correction algorithm<sup>17</sup> is used to prevent the unwanted exposure of pixels while the CCD is reading out.

Sixty-four fibers optics from the edge CXRS are coupled to a spectrometer with 400 mm  $f/2.8$  lenses and another Andor DU-897 E CCD. This spectrometer has two 400-mm focal length camera lenses with  $f/2.8$  and a 2160 lines/mm grating (Bunkou-Keiki CLP-400<sup>18</sup>). The dispersion is 0.012 nm/pixel at 500 nm. A pair of fibers viewing the identical radius are added together to improve the temporal resolution and positioned symmetrically on the detector to minimize offset of the wavelength due to aberrations of the spectrometer.

### III. ALIGNMENTS AND CALIBRATIONS

The alignment and focus of the spectrometer, CCD, and fiber optics are carried out using an Hg-Ne lamp. To calibrate the CX wavelengths of different impurity species, a set of pencil-style lamps (Hg, Ne, Kr, Ar, Xe) are used.

A careful optical alignment of the collection optics is critical for the data analysis and the deduction of unwanted contributions. A reference line produced by laser collimator on the midplane that extends along the path of the central neutral beam source is located. A grid screen is placed on this line, indicating the position and direction of the beam trajectory. With fibers backlit using a white source, the lens is adjusted again so that the images of the fibers focus on the desired positions along the reference plane. Figure 4 shows final image of all the fibers for the core CXRS. Irregularities in fiber illumination are due to uneven source distribution. The red line indicates the injection of tangential NBI. After aligned, the components are locked.

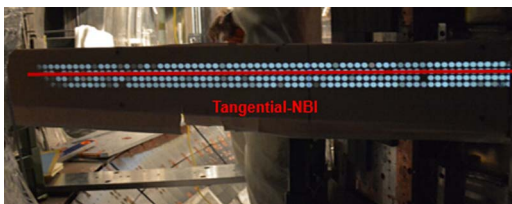


FIG. 4. Fiber images in vessel for core CXRS. Irregularities in fiber illumination were due to uneven source distribution.

The spatial locations of the sightlines are then located by back-illuminating the fibers with a laser and a calibration measurement arm. The position of the fiber images is measured on a set of planes along their paths. The path of each sightline is then located.

Absolute intensity calibration of each channel is performed inside the vessel via an integrating sphere source. A reflector is installed on the shutter blade to define a plane that is normal to the viewing sightlines with a laser. In this way, the viewing cone of one fiber is completely filled by the aperture of the sphere. The fiber is then illuminated by the sphere after removing the mirror and the light by the sphere is then recorded by the detector at the detected wavelengths.

### IV. SUMMARY

The CXRS and BES diagnostics had been developed for the coming 2014 campaign on EAST. Combining the measurements from the plasma core and the edge allows a full radial profile to be obtained. The simultaneous measurement of BES along the same sightlines provides the possibility for *in situ* calibration of CXRS signals. The simultaneous measurement of ion temperature, rotation, and density from multiple impurities help cross check the results. Deviations from the parabolic image of a straight entrance slit, which would lead to an apparent velocity, have been quantified by measurements with spectral lamps.

### ACKNOWLEDGMENTS

This work was supported by National Magnetic Confinement Fusion Science Program of China (Nos. 2011GB101004, 2011GB107003, 2012GB101001 and 2013GB112004), Natural Science Foundation of China (No. 11175208), and JSPS-NRF-NSFC A3 Foresight Program in the field of Plasma Physics (No. 11261140328).

<sup>1</sup>R. C. Isler, *Plasma Phys. Controlled Fusion* **36**, 171 (1994).

<sup>2</sup>R. J. Fonck *et al.*, *Phys. Rev. A* **29**, 3288 (1984).

<sup>3</sup>A. Kappatou *et al.*, *Rev. Sci. Instrum.* **83**, 10D519 (2012).

<sup>4</sup>M. von Hellermann *et al.*, *Rev. Sci. Instrum.* **77**, 10F516 (2006).

<sup>5</sup>I. O. Bespamyatnov *et al.*, *Rev. Sci. Instrum.* **81**, 10D709 (2010).

<sup>6</sup>R. Dux *et al.*, "Impurity density determination using charge exchange and beam emission spectroscopy at ASDEX Upgrade," in *39th EPS Conference on Plasma Physics and 16th International Congress on Plasma Physics*, Stockholm, Sweden, 2–6 July 2012.

<sup>7</sup>C. Chrystal *et al.*, *Rev. Sci. Instrum.* **83**, 10D501 (2012).

<sup>8</sup>Y. Xie *et al.*, *Rev. Sci. Instrum.* **85**, 02B315 (2014).

<sup>9</sup>Y. Li *et al.*, "The edge rotation and temperature diagnostic system on EAST tokamak," in *2012 Symposium on Photonics and Optoelectronics*, Shanghai, China, 21–23 May 2012.

<sup>10</sup>Y. Shi *et al.*, *Plasma Sci. Technol.* **12**, 11 (2010).

<sup>11</sup>M. G. von Hellermann, *et al.*, *Phys. Scr.* **T120**, 19 (2005).

<sup>12</sup>S. Zou *et al.*, National Institute for Fusion Science Data Series 69 (2001).

<sup>13</sup>M. Podesta *et al.*, *Nucl. Fusion* **52**, 033008 (2012).

<sup>14</sup>R. E. Bell, *Rev. Sci. Instrum.* **75**, 4158 (2004).

<sup>15</sup>R. E. Bell and F. Scotti, *Rev. Sci. Instrum.* **81**, 10D731 (2010).

<sup>16</sup>See <http://www.princetoninstruments.com/cms/index.php/ccd-primer/150-excelon-new-generation-ccd-technology> for information on the CCD technology.

<sup>17</sup>W. Ruyten, *Opt. Lett.* **24**, 878 (1999).

<sup>18</sup>M. Yoshinuma *et al.*, *Fusion Sci. Technol.* **58**, 103 (2010).